

# A wide characterization of paraffin-based fuels mixed with styrene-based thermoplastic polymers for hybrid propulsion

*Matteo Boiocchi\**, *Praskovia Milova\**, *Luciano Galfetti\**, *Luca Di Landro\** and *A.K. Golovko\*\**

*\*Politecnico di Milano, Aerospace Science and Technology Department*

*Via La Masa 34, I-20156 Milano, Italy*

*\*\*Siberian Branch of the Russian Academy of Sciences, Institute of Petroleum Chemistry*

*Tomsk, Russia*

## Abstract

In the framework of a long-term research activity focused on the development of high-performance solid fuels for hybrid rockets, paraffin-based fuels were investigated and characterized using two different pure paraffinic waxes and a styrene-based thermoplastic elastomer as strengthening material. The fuels were studied using differential scanning calorimetry (DSC) and thermo-gravimetric analysis (TGA-DTA). The viscosity of the melt layer, responsible for the entrainment effect, was investigated using a Couette viscosimeter. The storage modulus ( $G'$ ) was analyzed using a parallel-plate rheometer. The chemical composition of the pure paraffinic materials was studied using gas-chromatography (GC-MS) and mechanical properties through uniaxial tensile tests.

## 1. Introduction

Research activities performed at Stanford University at the beginning of the century showed that paraffin-based fuels for hybrid rockets burn at surface regression rates from three to four times those of conventional hybrid fuels [1-3]. For this reason paraffin-based materials have been proved to be very attractive fuels for hybrid rocket propulsion systems. These fuels form a thin, hydrodynamically unstable liquid layer on the melting surface of the fuel and the entrainment of droplets from the liquid-gas interface increases the rate of fuel mass transfer, leading to a much higher surface regression rates compared to that achieved using conventional polymeric fuels [4]. However, the main drawback of paraffin waxes is represented by low mechanical properties [5]. In order to develop a family of fuels, with ballistic and mechanical properties suitable for high-thrust class boosters, two paraffin-based fuels were investigated and characterized using two different pure paraffinic waxes and a styrene-based thermoplastic elastomer as strengthening material. A styrene-ethylene-butylene-styrene block copolymer grafted with maleic anhydride (SEBS-MA) [6], [7] was melted and mixed with the paraffin wax under nitrogen atmosphere to prevent oxidative phenomena. The thermal behavior of petroleum waxes (paraffin slack wax) and paraffin-based fuels was studied using differential scanning calorimetry (DSC) and thermo-gravimetric analysis (TGA-DTA) investigating the influence of the different paraffin wax properties. DSC data show two partially overlapping melting peaks (32–34°C and 53–54°C), and a third extended peak (243–273°C) linked to the evaporation/pyrolysis of the wax. The viscosity of the melt layer, main responsible for the entrainment effect, was investigated using a Couette viscosimeter; the storage modulus ( $G'$ ) was analyzed using a parallel-plate rheometer. All the mixtures containing SEBS-MA, show a rheological response supposedly affected by the storage time: three weeks of ageing cause an increase in viscosity between 110% and 25% linked with the rotational frequency. The chemical composition of the pure paraffinic materials was studied using gas-chromatography (GC), which was also applied for the analysis of the strengthened material ageing. Mechanical properties were investigated through uniaxial tensile tests in order to measure the influence of the thermoplastic polymer used.

## 2. Investigated materials

Paraffin waxes are a mixture of hydrocarbons, mainly normal alkanes. Carbon numbers span in the range approximately between 18 and 45. Paraffins are rather weak and brittle and for this reason, for applications requiring suitable mechanical properties, such as the solid fuel of a hybrid rocket engine, they are ill-suited. Research efforts are devoted to develop high performance materials with a greater stiffness and a greater elongation at break.

The first investigated paraffin was a commercial paraffin (GW) , supplied by an Italian Company, with a DSC melting point of 54.9°C. The second was a Russian product, available in the framework of a cooperation agreement between Politecnico di Milano and the Institute of Petroleum Chemistry of Tomsk, of the Siberian branch of the Russian Academy of Sciences. Its DSC melting point was measured to be 53.4 °C.

SEBS is a styrene-ethylene-butylene-styrene block copolymer, grafted with maleic anhydride (SEBS-MA), supplied by Sigma Aldrich.

Different compositions were manufactured and characterized, according to the list and the nomenclature of Table 1. The mixing between SEBS and wax was obtained firstly by melting a 50/50 % mixture under stirring at 110°C; when the mixture becomes homogeneous the last part of paraffin has to be added reducing the temperature at 90°C. The last ingredient to be added is carbon black. A good temperature control during all these operations is strictly needed in order to prevent a dissociation of maleic anhydride contained in SEBS-MA and at the same time to avoid the partial evaporation of the lighter carbon fractions contained into the paraffin wax. For paraffin-based mixtures, it is generally true that the higher is the temperature of the melt, the stronger is the shrinkage effect of the mixture into the mold during the cooling.

Table 1: Composition and density of studied pure paraffinic materials and SEBS-based blends.

<b>Fuel</b>	<b>Composition</b>	<b>Theoretical Density[g/cm<sup>3</sup>]</b>
GW	Gelly Wax	0.880
RW	Russian Wax	0.890
SEBS	Styrene 30% Maleic anhydride 2%	0.910
S05G	SEBS 5% GW 94% CB 1%	0.886
S10G	SEBS 10% GW 89% CB 1%	0.888
S15G	SEBS 15% GW 84% CB 1%	0.889
S15R	SEBS 15% RW 84% CB 1%	0.889
S20G	SEBS 20% GW 79% CB 1%	0.891
S30G	SEBS 30% GW 69% CB 1%	0.894

## 3. Differential Scanning Calorimetry

The Differential Scanning Calorimetry (DSC) measurements of the three pure waxes and the different mixtures were performed with a TA Instruments model 2010 CE thermal analyzer system. The calibration was performed with an Indium standard by normative; all the experiments were performed by using nitrogen gas (33 ml/min) as heating/cooling gas and tested at 10K/min as temperature ramp. All the sample tested where weighted by a Mettler Toledo electronic balance (0.1 mg accuracy) and the sample mass ranged between 2.4 and 2.7 mg.

Figure 1 shows the DSC scan of the GW and RW paraffin waxes used throughout this study. The scan shows the heating cycle, for which the lower transition temperature starting at about 28 °C, with a peak at 32°C and 36 °C for RW and GW respectively, corresponds to the pre-melting solid-solid transition. The higher temperature transition, the same for both the selected paraffins (peak at 53°C), is the melting transition. The high-temperature peaks occurs between 190°C and 210°C and they could be attributed to the gasification/decomposition process.

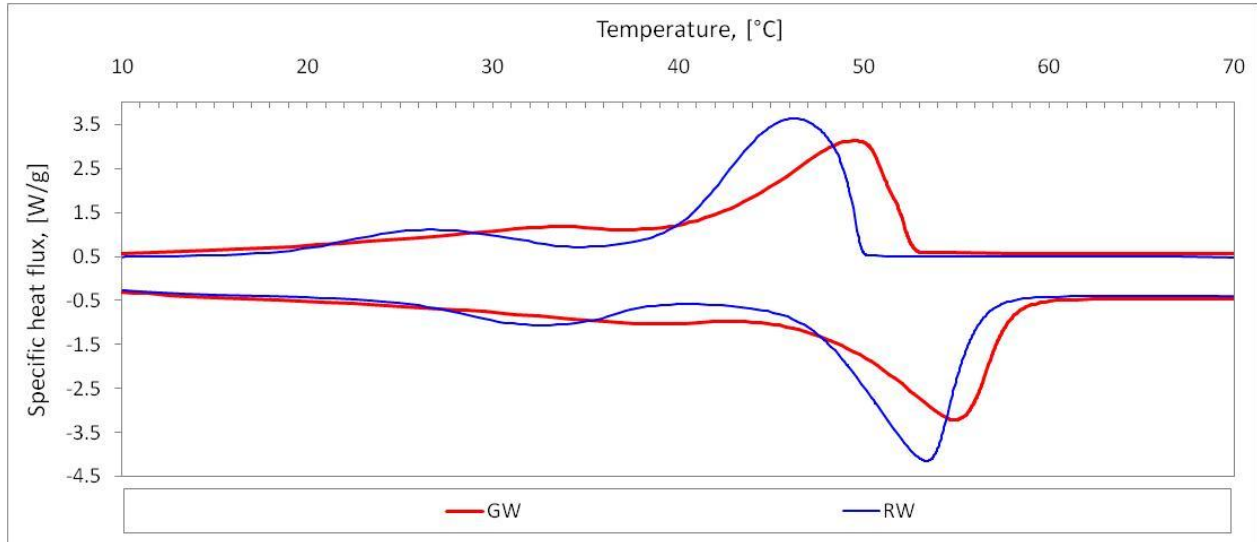


Figure 1: DSC scan of pure GW and RW waxes.

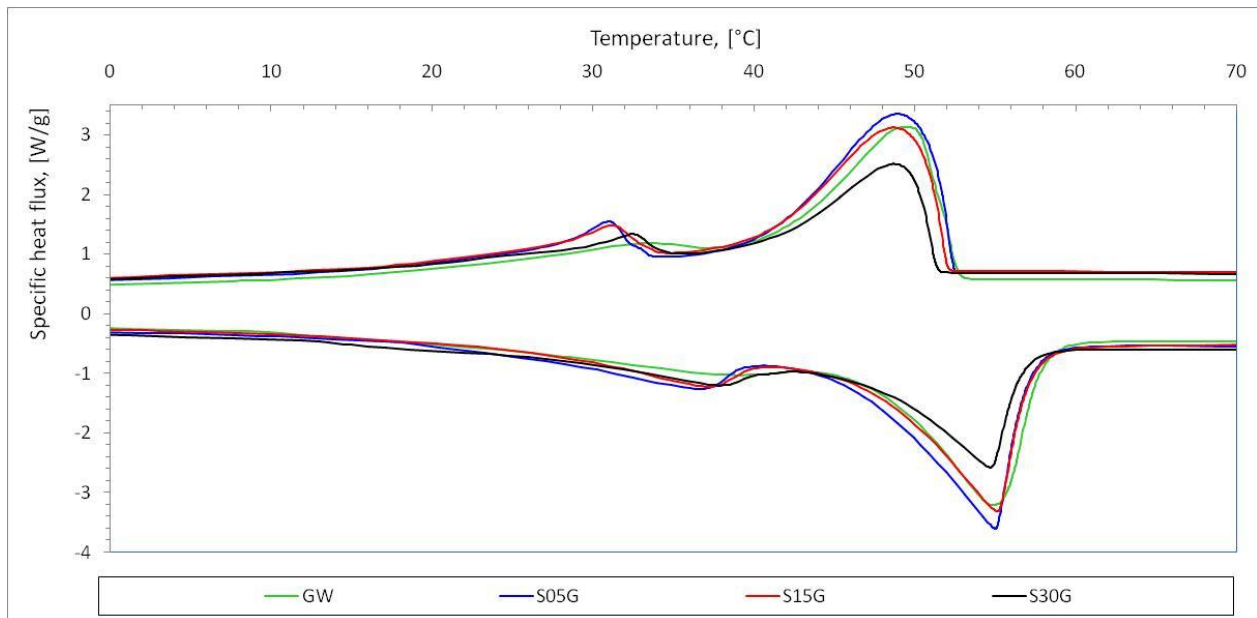


Figure 2: DSC thermographs of different GW-based formulations with three different SEBS concentrations.

Table 2: Parameters obtained from DSC measurements for paraffinic waxes ('T' temperature, ' $\Delta H$ ' specific enthalpy, 'm' melting, 'c' cooling)

Material	$T_{m,p} 1$ [°C]	$T_{m,p} 2$ [°C]	$\Delta H_m$ [J/g]	$T_{c,p} 1$ [°C]	$T_{c,p} 2$ [°C]	$\Delta H_c$ [J/g]
GW	39.1	54.9	219.1	33.6	49.5	199.4
RW	32.6	53.4	224.9	26.8	46.2	200.6
S05G	36.7	55.0	224.6	31.0	48.9	207.8
S15G	37.3	55.1	212.5	31.2	48.6	192.9
S30G	37.9	54.7	168.6	32.5	48.7	152.9

A comparison between DSC and TGA curves is shown in figures 3 and 4 for GW and RW pure waxes, respectively. In both figures the small shift in the first endothermic peak is due to the lower sensitivity of the TGA technique and to the difference in the use of the sample mass (2 mg in DSC vs. 16 mg in TGA). This first peak is due to the thermal decomposition in nitrogen atmosphere. The exothermic peak shown by the TGA curve when the test is performed in air is due to combustion of the sample.

The curves which show the mass loss (%) point out that the sample gasification occurs approximately in the range between 200 and 300 °C. The residual mass, at higher temperature, is due to ashes, hard to be oxidized.

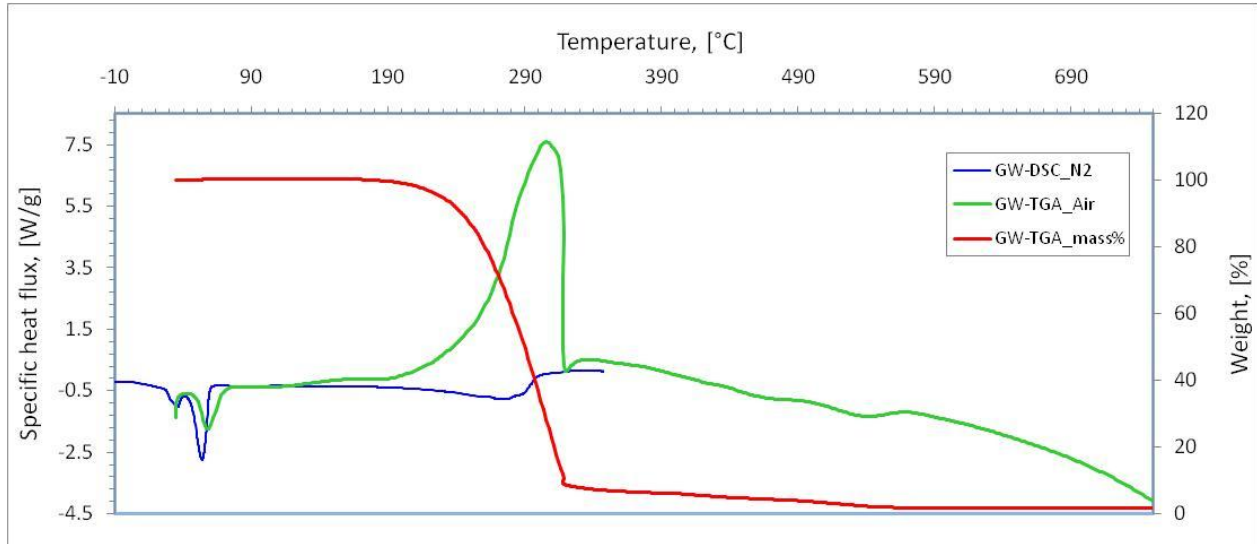


Figure 3: DSC scans in N<sub>2</sub> and air atmosphere overlapped to the TGA curve which shows the % mass loss. Pure GW material.

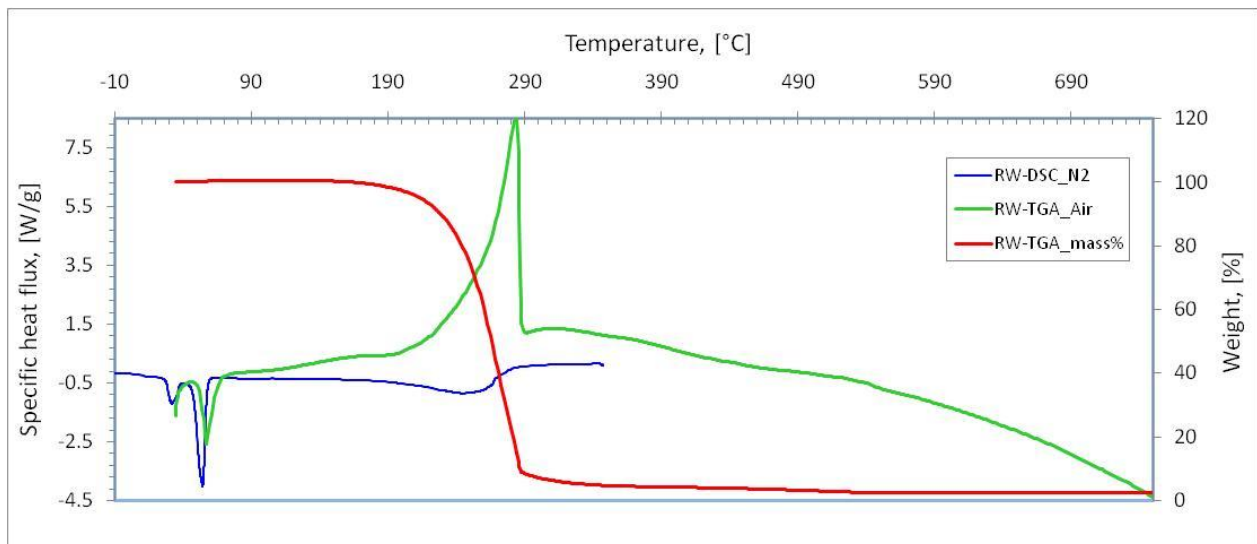


Figure 4: DSC scans in N<sub>2</sub> and air atmosphere overlapped to the TGA curve which shows the % mass loss. Pure RW material.

Figure 5 compares the exothermic peaks, measured in TGA tests, for the two GW and RW waxes. For RW the peak is narrower, meaning that oxidation reactions occur in a shorter time interval for RW. Further, the loss mass curve for S15G shows approximately at 300 °C a larger fraction of the residues, compared to that of the pure wax GW.

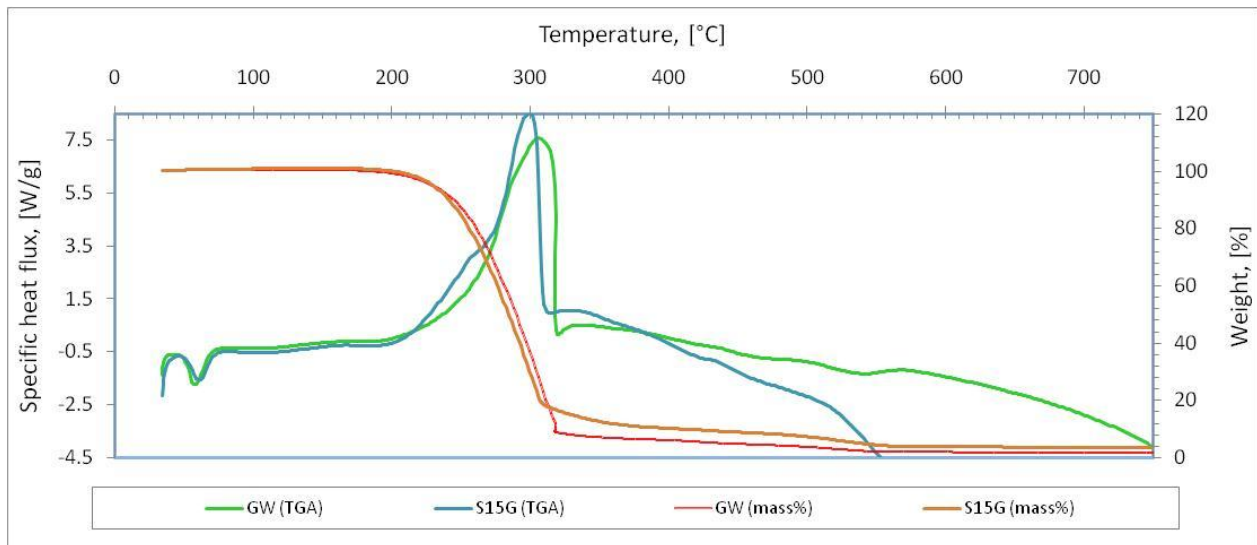


Figure 5: Comparison of the exothermic peaks for pure GW and RW waxes and mass loss curves for pure GW and S15G.

#### 4. Viscoelastic characterization

The rheological characterization of thermoplastic polymers and its blends is a complex subject that requires careful test design in order to obtain the information needed to meet the investigator's requirements. In order to obtain the viscoelastic behaviour of the investigated formulations a rotational rheometer was used. All the experiments were carried out by a *Rheometrics Dynamic Analyzer RDA II* using a Couette apparatus for viscosity measurements on melted materials and a parallel plate apparatus to study the elastic and storage moduli ( $G'$ ,  $G''$ ).

##### 4.1 Dynamic viscosity

Figure 6 shows the viscosity behaviour of a melted SEBS-based blend (SEBS 15%, Wax 84%, CB 1%) tested at 85°C, at different rates and in two different ageing conditions. The sample S15G (fresh) was tested 24 hours after preparation. The same mixture was tested in the same conditions after three weeks in which the sample was stored at 25°C.

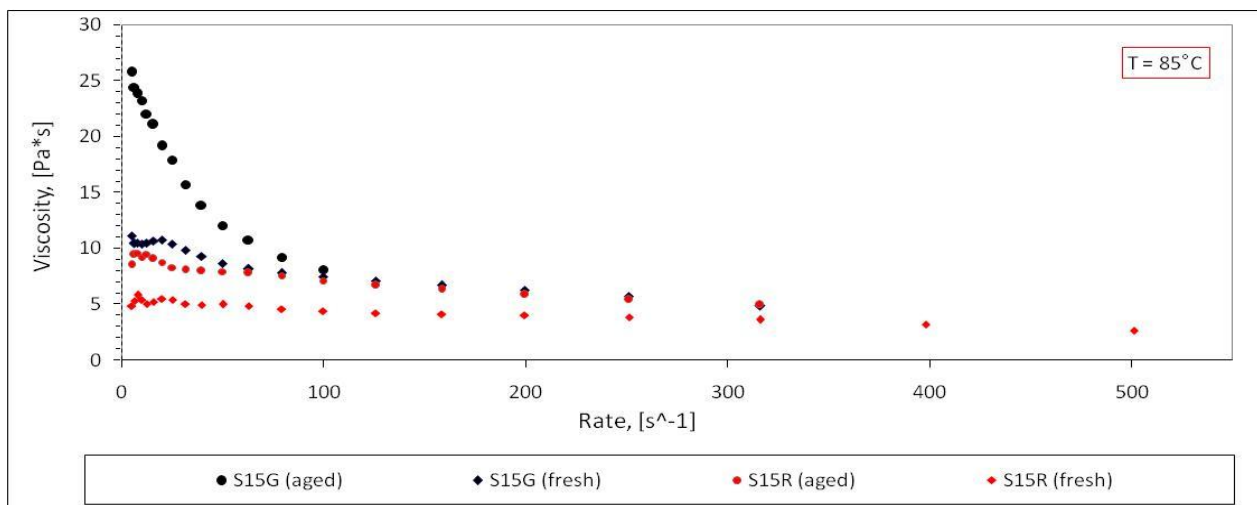


Figure 6: Trend of viscosity for fresh and aged samples of S15G material. Temperature of the tests: 85 °C.

The ageing effect of SEBS-based mixtures containing both GW and RW, is shown in Figure 6. Considering low values of rate (less than  $100 \text{ s}^{-1}$ ) the viscosity of aged samples is higher than that of fresh samples for both the different kind of paraffins. As the rate increases the viscosity decreases; the RW-based formulation shows a lower viscosity than GW-based formulation.

Figure 7, 8, 9 and 10 shows the viscosimetric behaviour of the same previous composition (fresh and aged) investigated in the temperature range  $85 - 165 \text{ }^\circ\text{C}$ .

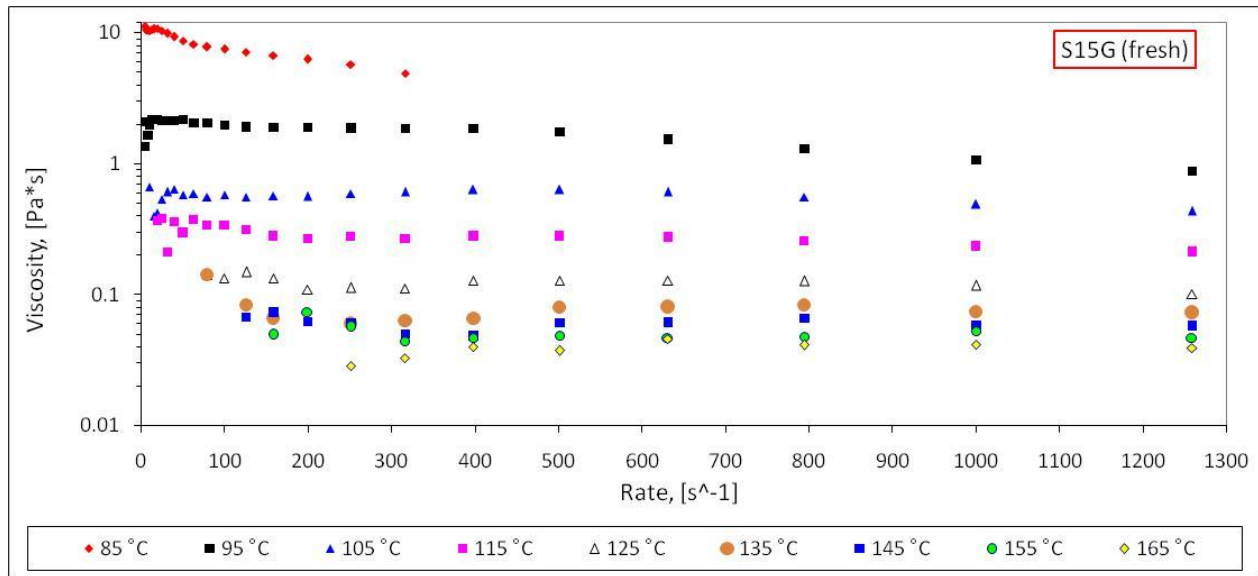


Figure 7: Temperature scan of viscosity in the range  $85 \text{ }^\circ\text{C} - 165 \text{ }^\circ\text{C}$  for fresh samples of S15G material.

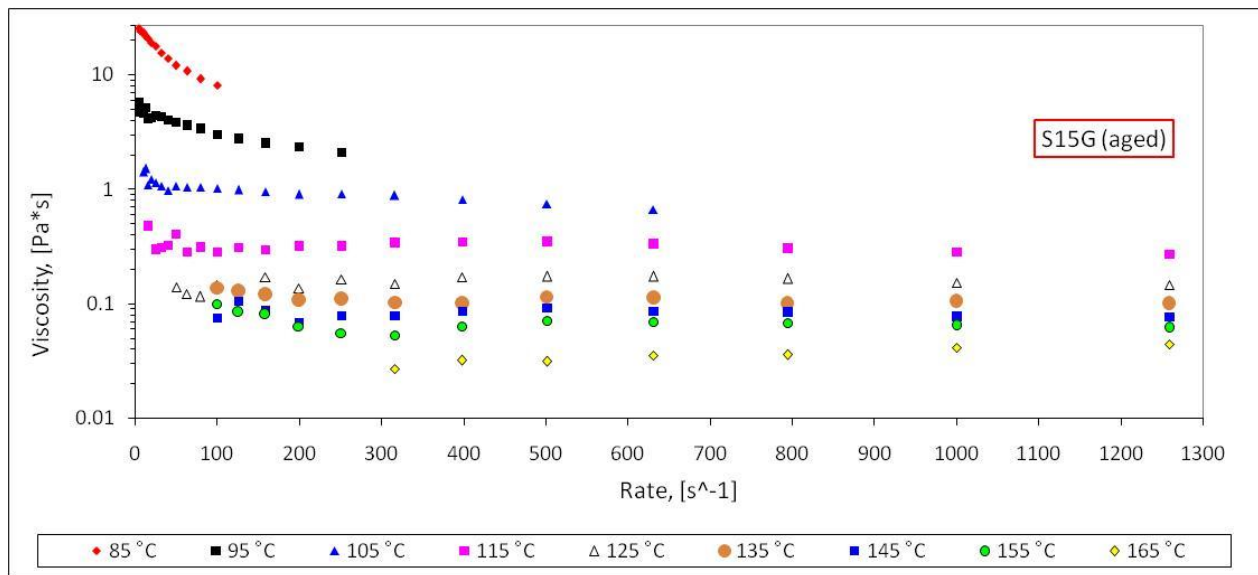


Figure 8: Temperature scan of viscosity in the range  $85 \text{ }^\circ\text{C} - 165 \text{ }^\circ\text{C}$  for aged samples of S15G material.

The viscosity of the aged samples was higher than that of the fresh formulations at low temperatures but this difference becomes less clear as the temperature of the melt is increasing. Considering the aged formulation tested at  $85, 95$  and  $105 \text{ }^\circ\text{C}$ , tests were interrupted (at  $100, 250$  and  $630 \text{ s}^{-1}$  respectively) because the limit of maximum torque was reached. The measured maximum torque values for fresh formulations were always lower than the superimposed limit; for this reason the graphs were not interrupted in advance.

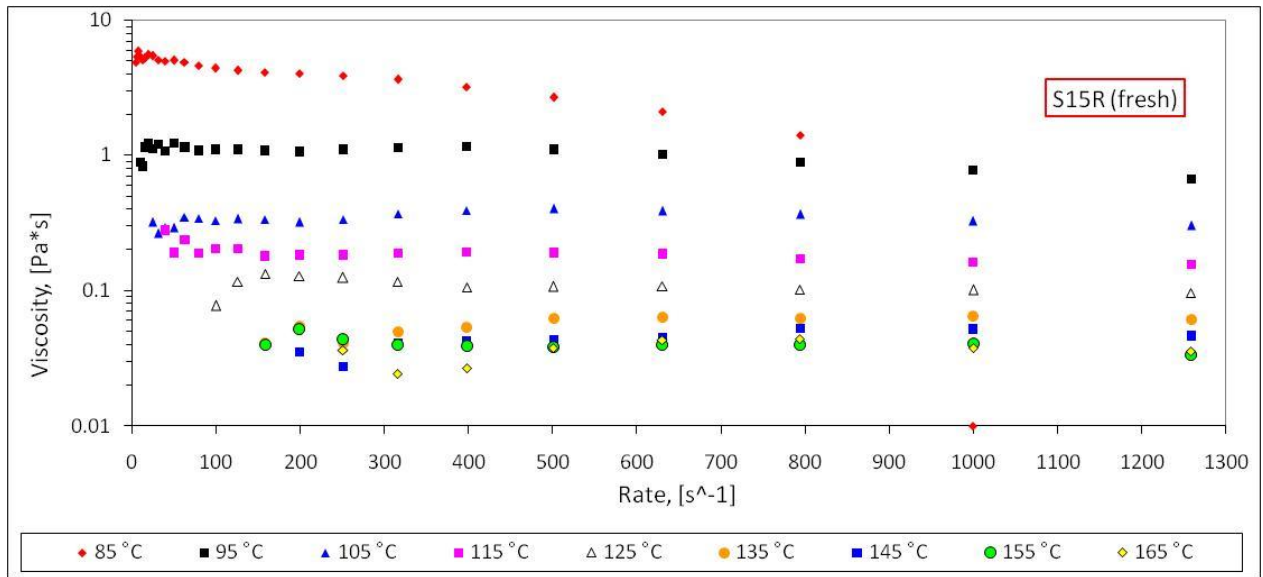


Figure 9: Temperature scan of viscosity in the range 85 °C – 165 °C for fresh samples of S15R material.

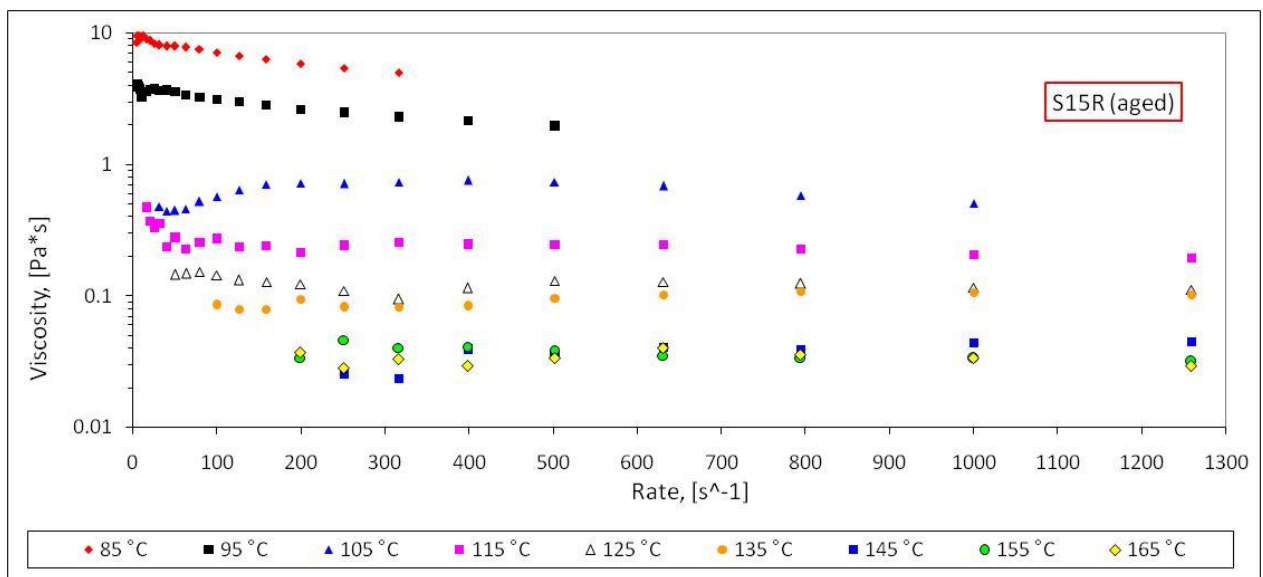


Figure 10: Temperature scan of viscosity in the range 85 °C – 165 °C for aged samples of S15R material.

A comparison between two families of SEBS-based blends containing GW and RW waxes was made; a clear trend was observed. At same experimental conditions, like temperature of the melt and rate of the Couette apparatus, Table 3 points out that RW-based blends have a lower viscosity than GW-based mixtures.

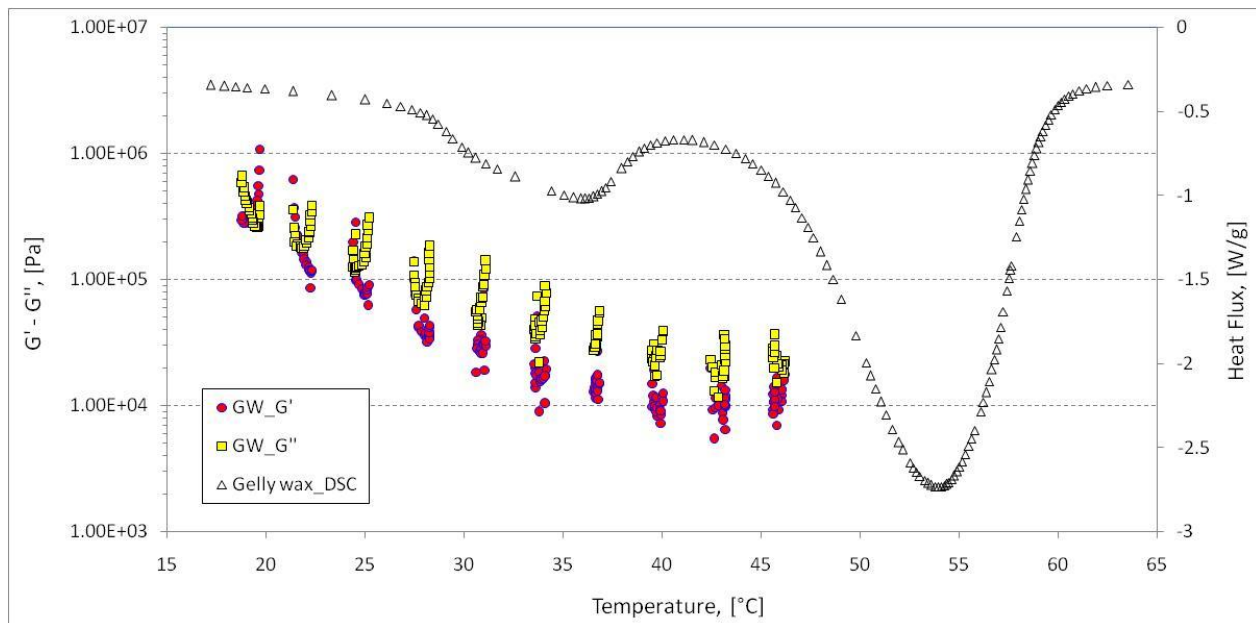
Table 3: Viscosity values obtained with Couette rheometer tests at  $1000 \text{ s}^{-1}$ , ordered in decreasing values.

Mixture	Viscosity values @ $1000 \text{ s}^{-1}$							
Temperature	95	105	115	125	135	145	155	165
S15G fresh	1.071	0.491	0.236	0.118	0.074	0.059	0.053	0.042
S15G aged	-	-	0.285	0.153	0.106	0.078	0.064	0.041
S15R fresh	0.777	0.327	0.162	0.101	0.064	0.052	0.041	0.038
S15R aged	-	0.508	0.207	0.116	0.105	0.044	0.033	0.034

## 4.2 Rheology

A preliminary investigation on the rheological behaviour of the selected materials was performed by determining the elastic moduli response by variation of the percentage strain value. A value of percentage strain of 1% was selected as a good trade-off between the needed stress/strain linearity and the sensitivity of the test bench.

Figures 11 and 12 show the trend of  $G'$  and  $G''$  for pure wax GW and RW respectively. The shift occurring between the endothermic peak pointed out by DSC test and the beginning of  $G'$  sharp decrease (and symmetrically the sharp increase of  $G''$ ) has to be linked to the different mass of the samples (2mg vs. 2 g). Different masses are characterized by different thermal inertia.

Figure 11: Trend of  $G'$  and  $G''$  vs. T for pure wax GW.



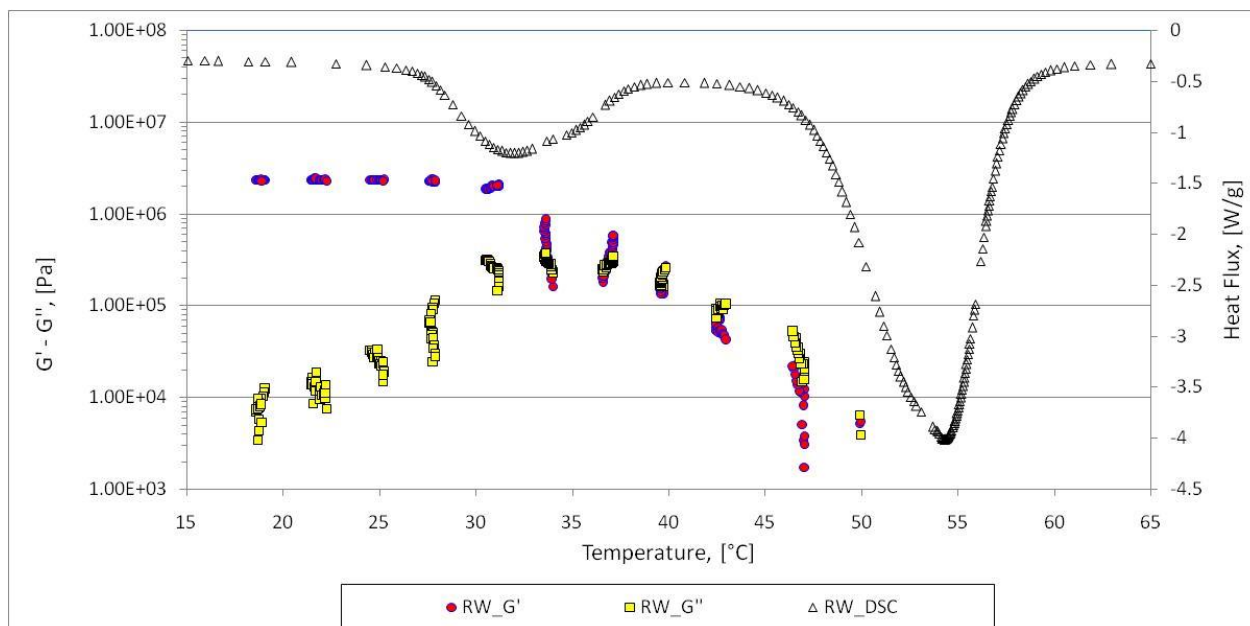


Figure 12: Trend of  $G'$  and  $G''$  vs.  $T$  for pure wax RW.

The comparison of the relative position of the endothermic peaks given by DSC tests and the behavior of  $G'$  and  $G''$  trends for pure GW and fresh S15G allows appreciating how the different phases of GW melting affect  $G'$  and  $G''$  behavior.

Figure 13 shows the behavior of fresh and aged SEBS-based formulation (SEBS 15%, GW 84%, CB 1%), in terms of  $G'$  and  $G''$ , compared with the DSC trace.

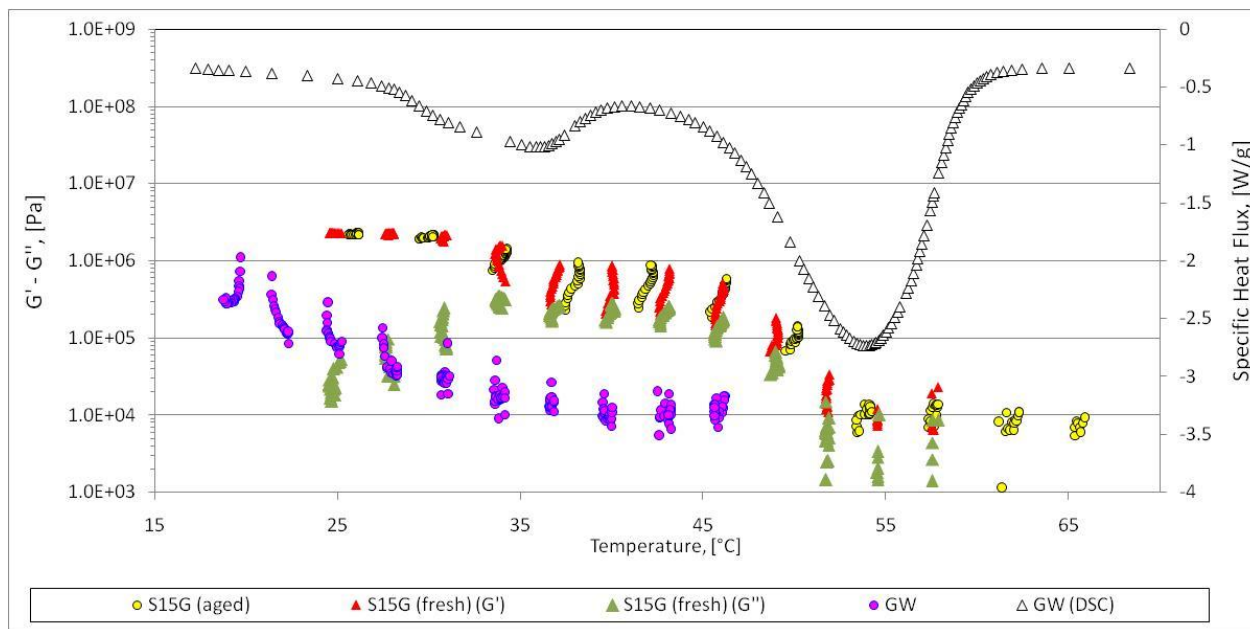


Figure 13: Trend of  $G'$  and  $G''$  for pure GW compared with S15G blend fresh and aged.

Considering SEBS-containing formulations (5%, 15% and 30%) thermographs, they seem to be characterized by the same melting temperature of pure GW. Figure 2 shows that the melting temperature increases as the SEBS fraction increases. DSC test is not able to detect a change in phase of this kind of polymer because probably it is an amorphous polymer. Non-ordered copolymers are generally amorphous, while copolymers made of long blocks of both co-monomer types can display the same crystallinity characteristics typical of both homopolymers.

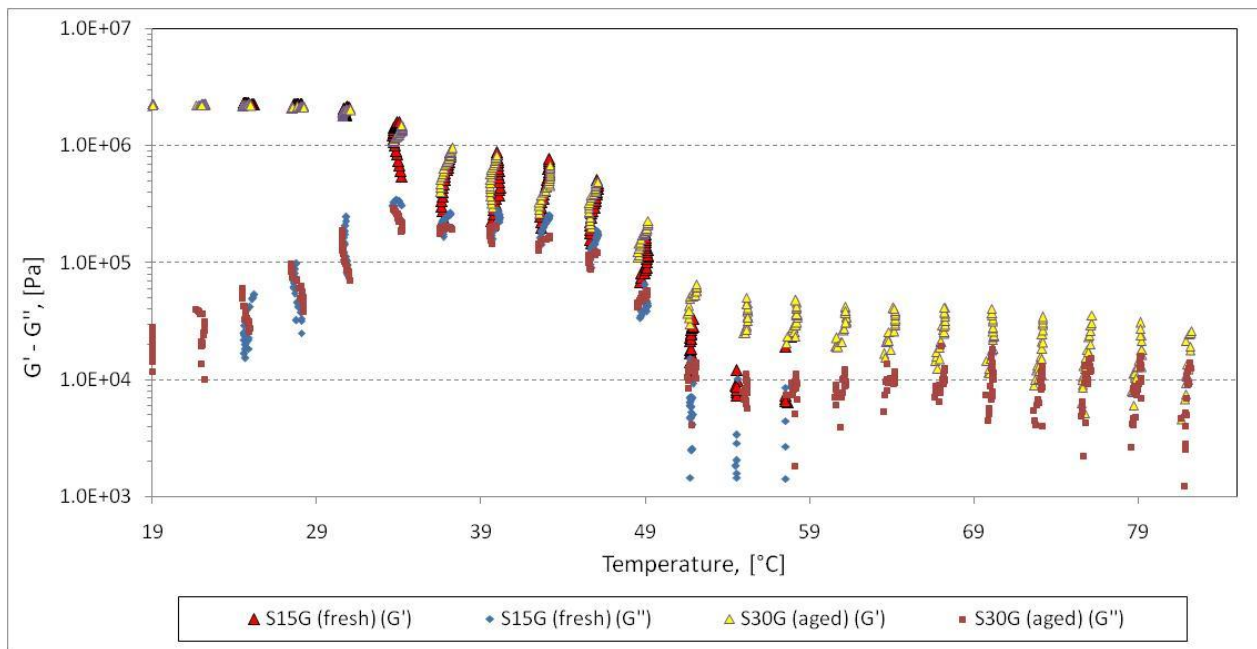


Figure 14: Trend of  $G'$  and  $G''$  for S15G blend samples, fresh and aged.

DSC tests point out that the peak where GW melting occurs is at 54  $^{\circ}C$ . If the mass fraction amount of the polymer is larger than 15%, the mixture is liquid at larger temperatures ( $G'$  cannot be measured). This trend negatively affects the regression rate behavior.

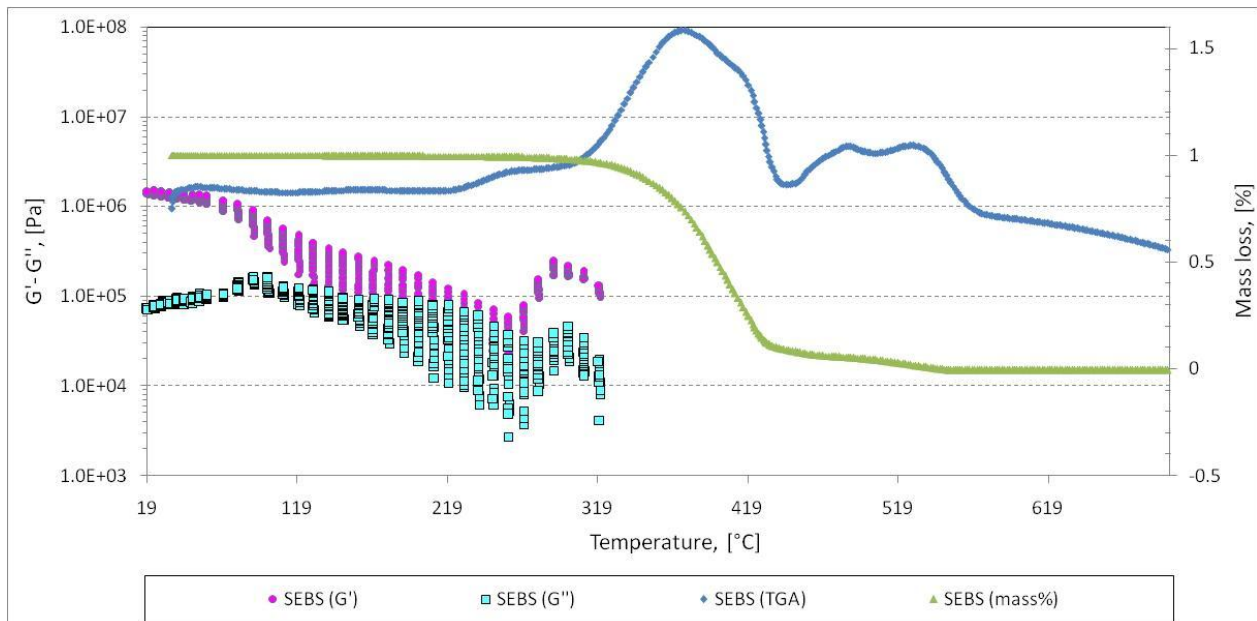


Figure 15: trend of  $G'$  and  $G''$  for a sample of pure SEBS compared with its TGA trace

Figure 15 shows the  $G'$  and  $G''$  behaviour of SEBS tested between 19 $^{\circ}C$  and 321 $^{\circ}C$ . A TGA with a percentage mass loss was reported to correctly identify the start of the thermal degradation of the sample. TGA trace indicates that in the range 220 $^{\circ}C$  – 310 $^{\circ}C$  a little exothermic peak occurs and it is linked with the final part of the elastic modulus trace. The increase in  $G'$  could be explained considering the test method implemented and the chemical composition of the sample. According with the usual method, a sample disk of material (25 mm diameter, 1.5 mm thickness) was placed in a hoven in which it was heated by an air flux. At high temperature the annular surface of sample directly

exposed to the air flux could react by thermo-oxidative reactions leading to a molecular structure modification of the polymer. Another reason is referred to the maleic anhydride content of the polymer. SEBS-MA is used to increase the mechanical properties of epoxy resins because of the creation of strong chemical bonds between the epoxy ring and the maleic anhydride ring. The well verified high chemical reactivity of maleic anhydride at low temperatures could explain little exothermic peak observed.

## 5. Mechanical properties

The mechanical characterization was carried out on pure GW and its blends with different amount of SEBS (5, 10, 15, 20 and 30%) at the speed of 0.5 and 50 mm/min. Material samples were obtained by casting the melted mixture into a mould designed according to UNI-EN-ISO 527 norm for plastic materials. Material testing was performed with a PC-controlled uniaxial tensile test machine equipped with a load cell of 1KN (Instron Series 4302). Elastic modulus has been calculated in both methods described in the reference norm and no significant differences have been pointed out.

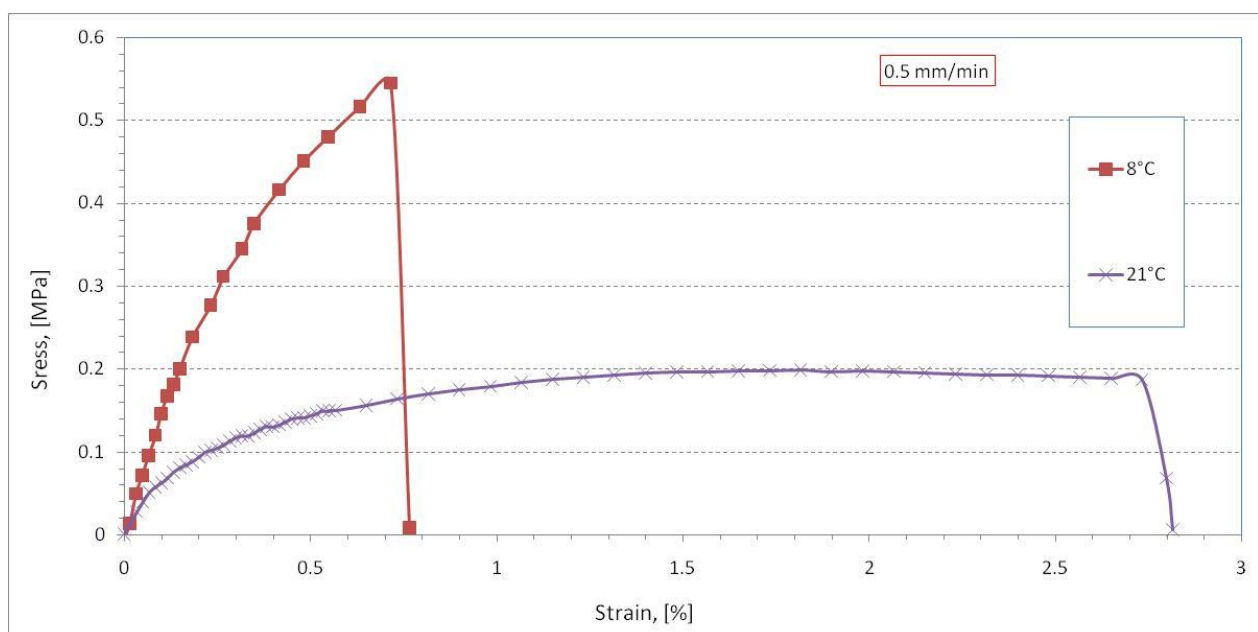


Figure 17: influence of the temperature on maximum load and elongation at break for pure GW sample

Figure 17 shows the influence of the temperature of the pure GW samples on maximum load (which falls from 0.54 MPa to 0.2 MPa) and specularly, on the value of elongation at break (which increase from 0.7 % to 2.7%). A possible explanation of this strong sensitivity to the temperature could be linked with the softening of the material starting at 15°C (See Figure 1: first soft endothermic peak).

Considering SEBS-based samples, as it can be seen in Figure 18, higher is the polymer fraction higher is the elongation at break. Materials with a polymer content lower than 15% (S05G and S10G sample) shows a behavior typical of rigid and brittle materials. As the SEBS mass fraction increases the elongation at break increases with a not linear trend.

Table 4: Young modulus obtained with tensile tests at -19°C, 8°C and 0.5, 50 mm/min for SEBS containing formulations

Blend Rate / T <sub>storage</sub> [mm/min] / [°C]	Young Modulus [MPa] / Standard Deviation [MPa]					
	GW	S05G	S10G	S15G	S20G	S30G
0.5 / 8	119.2 ± 17.32	123.1 ± 8.0	127.1 ± 1.1	106.7 ± 12.2	86.8 ± 2.1	75.3 ± 5.7
0.5 / -19	-	143.1 ± 17.7	141.7 ± 16.1	163.4 ± 12.3	130.6 ± 5.2	126.2 ± 6.5
50 / 8	-	246.1 ± 23.6	252.8 ± 19.2	211.7 ± 14.6	200.1 ± 4.2	162.6 ± 11.0
50 / -19	-	334.5 ± 13.9	327.4 ± 36.1	320.7 ± 14.2	299.4 ± 16.6	269.8 ± 2.3

It's interesting to note that a higher content of thermoplastic polymer results in decrease of the Young Modulus. A more significant decrease of the Young Modulus (51-63%) is observed when the fuel temperature is higher (in the case of this work it's 8 °C) and a lower decrease (13-24%) – when the temperature is low (-19 °C).

There is a clear evidence that the Young Modulus (See Figure 19) values are higher for each formulation when the sample temperature is decreased (from 8 °C to -19 °C).

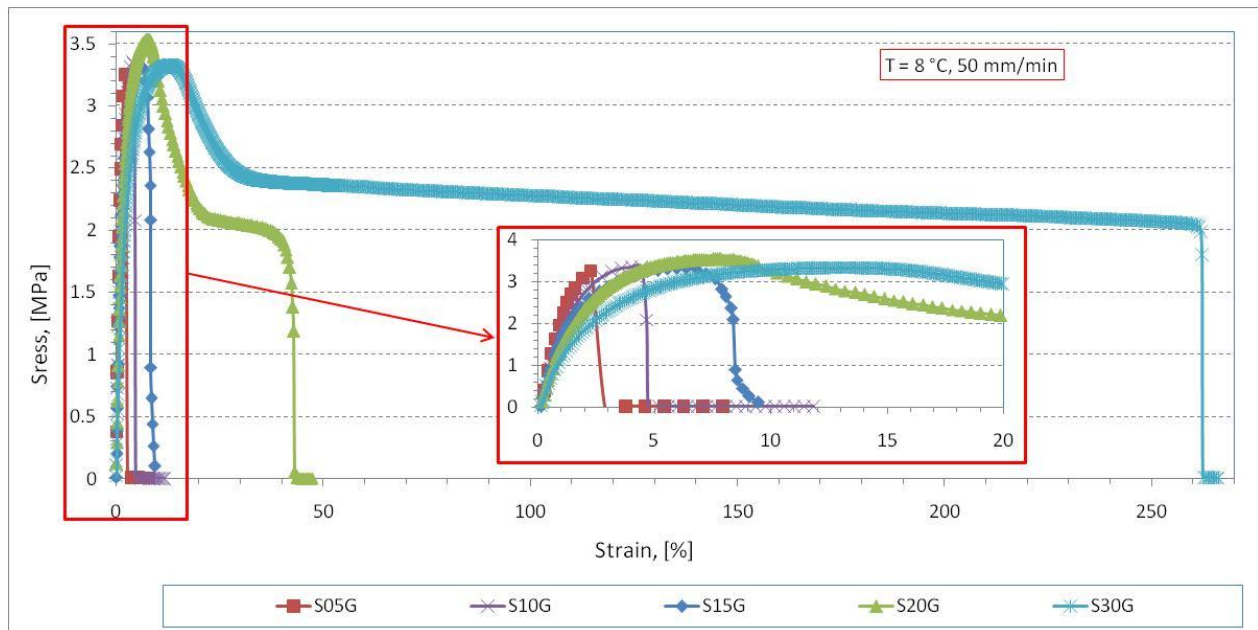


Figure 18: effect of polymer's mass fraction on the elongation at break

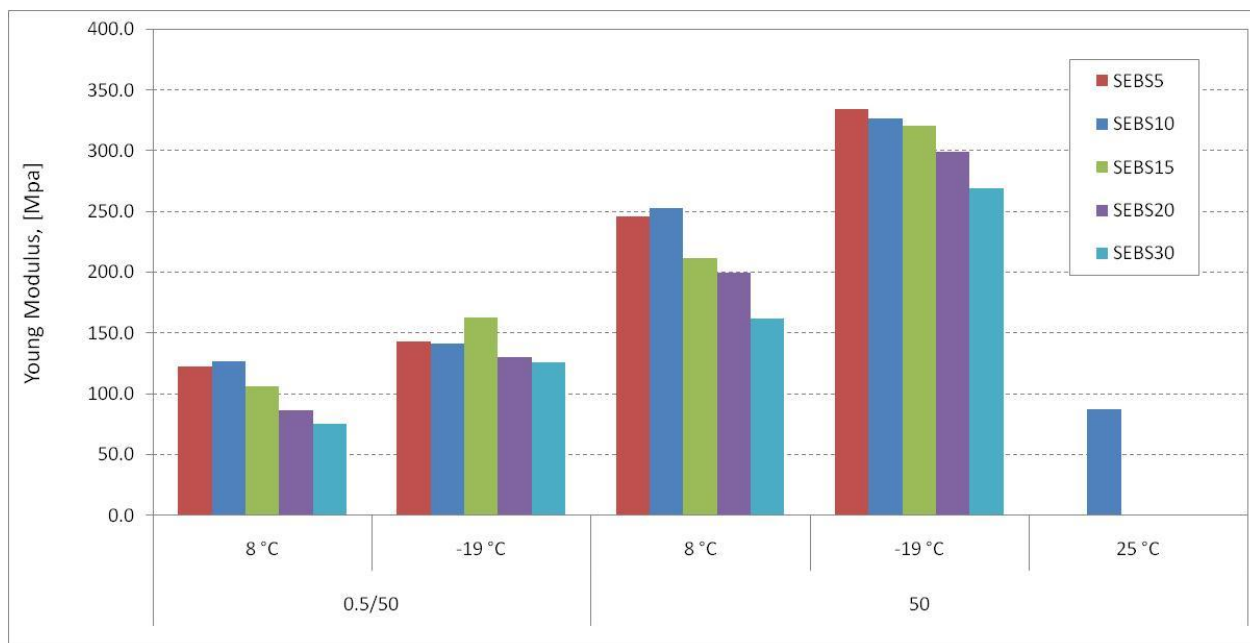


Figure 19: Young Modulus trend of SEBS-based formulations with the temperature and elongation speed

## 7. Conclusions

Paraffin waxes are inexpensive materials that are soft, weak and brittle. These properties provide limited performance when exposed to even small load. The need to significantly increase the mechanical properties of waxes is important for specific applications, such as the use of these materials in hybrid rockets propulsion systems. In addition waxes soften at quite low temperatures, further limiting their potential applications. In this study the behaviour of two pure waxes and their blends with a styrene-ethylene-butylene-styrene block copolymer, grafted with maleic anhydride, were investigated under a broad range of conditions.

The thermal behavior was studied using DSC and TGA-DTA, investigating the influence of the different paraffin wax properties. DSC data show two partially overlapping melting peaks (32 - 34°C and 53 - 54°C), and a third extended peak (243 - 273°C) linked to the evaporation/pyrolysis of the wax. The viscosity of the melt layer, main responsible for the entrainment effect, was investigated using a Couette viscosimeter, while the storage modulus ( $G'$ ) was measured using a parallel-plate rheometer. All the mixtures containing SEBS-MA, show a rheological response affected by the storage time: three weeks of ageing cause an increase in viscosity between 110% and 25% linked with the rotational frequency. A clear link between the decreasing of elastic modulus  $G'$  for all the studied formulations and the thermal behavior clarified by DSC tests was pointed out. Mechanical properties were investigated through uniaxial tensile tests in order to measure the influence of the thermoplastic polymer used. A strong influence of temperature of the sample and of SEBS mass fraction on maximum load and elongation at break was observed.

## References

- [1] Karabeyoglu, M.A., Cantwell, B.J., and Altman, D. 2001. Development and Testing of Paraffin-Based Hybrid Rocket Fuels. *37<sup>th</sup> AIAA/ASME/SAE/ASEE Joint Propulsion Conference and Exhibit*, Salt Lake City, Utah. AIAA Paper 2001-4503.
- [2] Karabeyoglu, M.A., Ziliac, G., Cantwell, B.J., DeZilwa, S., and Castellucci, P. 2004. Scale-Up Tests of High Regression Rate Paraffin-Based Hybrid Rocket Fuels. *Journal of Propulsion and Power*, Vol. 20, No. 6, pp. 1037–1045.
- [3] Chiaverini, M.J., Serin, N., Johnson, D., Lu, Y.C., Kuo, K.K. and Risha, G.A. 2000. Regression Rate Behavior of Hybrid Rocket Solid Fuels. *Journal of Propulsion and Power*, Vol. 16, No. 1, pp. 125–132.
- [4] Karabeyoglu, M.A. and Cantwell, B.J. 2002. Combustion of Liquefying Hybrid Propellants: Part 2, Stability of Liquid Films. *Journal of Propulsion and Power*, Vol. 18, No. 3, pp. 621–630.
- [5] Maruyama, S., Ishiguro, T., Shinohara, K. and Nakagawa, I. 2011. Study on Mechanical Characteristics of Paraffin-Based Fuel. *47<sup>th</sup> AIAA/ASME/SAE/ASEE Joint Propulsion Conference & Exhibit*, 31 July-3 August, San Diego, CA.
- [6] Kim J.K., Paglicawan M.A., and Balasubramanian M. 2006. Viscoelastic and Gelation Studies of SEBS Thermoplastic Elastomer in Different Hydrocarbon Oils. *Macromolecular Research*, Vol. 14, No. 3, pp. 365-372.
- [7] Zhang Q., Song S., Feng J., and P. Wu. 2012. A New Strategy to Prepare Polymer Composites with Versatile Shape Memory Properties. *Journal of Materials Chemistry*, Vol. 22, pp. 24776.